Available online at www.sciencedirect.com

SCIENCE DIRECT®

Journal of Organometallic Chemistry 675 (2003) 84–90

Journal of Organometallic Chemistry

www.elsevier.com/locate/jorganchem

Organosilyl derivatives of trivacant tungstophosphate of general formula α-A-$[PW_9O_{34}(RSiO)_3(RSi)]^{3-}$ Synthesis and structure determination by X-ray crystallography

Jingyang Niu *, Mingxue Li, Jingping Wang

School of Chemistry and Chemical Engineering, Henan University, Kaifeng 475001, PR China

Received 17 September 2002; received in revised form 25 March 2003; accepted 27 March 2003

Abstract

In the presence of NBu^n_4Br acting as phase-transfer reagent, organosilicon trichloride $RSiCl_3$ reacts in acetonitrile with the trivacant tungstophosphate sodium salt β-A-$Na_8H[PW_9O_{34}]\cdot24\ H_2O$ to give hybrid organosilyl polyoxotungstate derivatives α-A-$[NBu^n_4]_3[PW_9O_{34}(RSiO)_3(RSi)]$ ($R = C_2H_3$ (**1**), CH_3 (**2**)). These compounds are characterized by X-ray crystallography. Each of the two hybrid anions consists of one α-A-$PW_9O_{34}^{9-}$ framework on which is grafted by three RSiO groups through six Si–O–W bridges, each of which is attached to the fourth RSi through three Si–O–Si bridges. Both hybrid anions become saturated, close cage structure and display C_{3v} symmetry.

Keywords: Trivacant heterpolyanion; Organosilicon; Synthesis; Crystal structure

1. Introduction

The synthesis and characterization of new derivatized polyoxometalates are of current interest due to the potential and developed applications of these substances in many fields, including environmentally benign catalytic processes and antiviral chemotherapies [1–4]. In particular, organometallic derivatives of polyoxometalates have potential use as pharmaceuticals [4] and as phasing agents in the X-ray crystallography of proteins [5,6]. The reactivity of polyvacant polytungstates with organochlorostannanes [7–10] and organophosphonic acids [11] has been systematically investigated. In addition, the organosilyl derivatives of divacant lacunary anion γ-$PW_{10}O_{36}$ [7–12] and the preparation of POM-based macromolecules from the divacant POMs [13–15] have also been reported by Thouvenot and coworkers. Researches on the reaction of polyvacant polytungstates with organohalogenosilanes, however, are still limited [16,17]. To the best of our knowledge, X-ray crystal structure of α-A-$[NBu^n_4]_3[PW_9O_{34}(RSiO)_3(RSi)]$ which is close cage structure has not been reported. The present paper reports the synthesis and detailed structural description of two organosilyl derivatives from the lacunary anion β-A-$[PW_9O_{34}]^{9-}$ by X-ray single-crystal structure determination.

2. Results and discussion

2.1. Synthesis

Different synthetic approaches were attempted. Taken together, a conclusion was made that the reaction of $RSiCl_3$ with β-PW_9 in aqueous solution was unsuccessful. By systematically varying the experimental conditions, in the end, the reaction in acetonitrile is satisfactory. Unfortunately, the quality of all crystals obtained by evaporation of CH_3CN at room temperature is not pretty good because of the too rapid evaporation speed of CH_3CN. Therefore, by changing different solvents, at last, we obtained the suitable crystals for X-ray single crystal diffraction analysis by the slow evaporation of dimethylformamide (DMF)

---

* Corresponding author. Tel.: +86-378-2192443; fax: +86-378-2853650.

E-mail address: jyniu@henu.edu.cn (J. Niu).

0022-328X/03/$ - see front matter © 2003 Elsevier Science B.V. All rights reserved.
doi:10.1016/S0022-328X(03)00252-3

solvent. In addition, the structures of the title compounds confirm that they contain A-PW_9 building block which is A, α, not A, β. Other else, RSiO groups are incorporated into lacunary Keggin polytungstate structure, which appears that the fixation of RSiO groups induce a β → α isomerization of the $PW_9O_{34}^{9-}$ structure. This effect also exists in the course of formation of α-A-$[PW_9O_{34}(RPO)_2]^{5-}$ [11] and α-A-$[(PhSnOH)_3(PW_9O_{34})_2]^{12-}$ [7].

2.2. IR Spectra

The observed frequencies and tentative assignments of the main IR absorption bands for α-$[NBu^n_4]_4[PW_{12}O_{40}]$ (denoted as α-PW_{12}) [18], β-PW_9 [19] and the title compounds **1** and **2** are given in Table 1.

Infrared spectra of the title compounds are very similar. The low-wavenumber part ($v < 1000$ cm^{-1}) is characteristic of the polyoxometalate framework [20]. The stretching vibrational bands [ν_{as}(W–O_d) and ν_{as}(W–O_c–W)] are shifted to higher frequency, compared to those of the starting trivacant β-A-$[PW_9O_{34}]^{9-}$ anion. This effect is attributed to a partial saturation of the polyoxometallic moiety through the fixation of RSiO units. However, replacement of RSi^{3+} in the polyanions, which leads to the lower structural symmetry of the title anions in comparison with that of α-PW_{12}, results to the vibrational peaks of the ν_{as}(W–O_d) and ν_{as}(W–O_c–W) to split. At the same time, the compound **1** exhibits infrared bands at 3063, 1652, 1485, 1458, 1275, 1126, 732 cm^{-1}, indicative of C_2H_3Si group retention and the compound **2** exhibits infrared bands at 1262, 1123, 766 cm^{-1}, indicative of CH_3Si group retention.

2.3. UV Spectra

The samples all reveal two peaks at 198 and 264 nm for **1**, 199 and 265 nm for **2** and 200 and 265 nm for α-PW_{12}, respectively. The intense absorption band at ca. 260 nm is a characteristic of the 12-heteropoly tungstophosphate and has been attributed as $O_{b(c)} \rightarrow W$ charge transfer band; the higher energy band at 200 nm has been assigned to $O_d \rightarrow W$ charge transfer band. Absorption intensity between **1** and **2** is different. This may be a result of the differences in the properties of ethyl and methyl groups. In addition, absorption intensity of both **1** and **2** is weaker than that of α-PW_{12}, which arises in part from their lower symmetry compared to α-PW_{12}. In a word, the spectra of the title complexes in the range 190–400 nm are similar to those of α-PW_{12} and different from that of β-PW_9. This indicates that a close frame structure has been reformed by the reaction of RSi groups with β-PW_9, which is consistent with the results of IR spectra.

Table 1
Infrared data (cm^{-1}) for α-PW_{12}, β-PW_9, **1** and **2**

Complex	ν_{as}(P–O_a)	ν_{as}(W–O_d)	ν_{as}(W–O_b–W)	ν_{as}(W–O_c–W)
α-PW_{12}	1080s 1025w	987sh 976s	895s	810vs
β-PW_9	1056s 1014w	931vs	884m 815s	762s
1	1039w 1008sh	976sh 959vs 946s	868vs	818s
2	1037w 1001sh	974sh 959vs 944vs	867s	838m 813vs

O_a is bound to the central P atoms; O_b atoms are shared by two W atoms of different W_3O_{13} units; O_c atoms are shared by two atoms from the same Mo_3O_{13} unit; O_d is the terminal oxygen atom combined with only one W atom.

2.4. Thermal stability

Thermal stability of the title complexes has been studied by means of thermogravimetric and differential thermal measurements. TG curve of α-A-$[NBu^n_4]_3$-$[PW_9O_{34}(C_2H_3SiO)_3(C_2H_3Si)]$ exhibits two stages for loss of weight. The first weight loss of 23.19% occurs between 363.4 and 464.1 °C, corresponding to the loss of organic ammonium (calc. 22.68%); the second weight loss of 3.41% occurs between 464.1 and 543.4 °C, resulting from the loss of ethyl group (calc. 3.37%). One endothermal peak is observed at 378.6 °C (assigned as C–Si cracked) in DTA curve. A stronger exothermal peak is observed in DTA curve at 417.9 °C, which could arise from the decomposition of the framework of **1**. These results illustrate that the framework of the complex **1** decomposes at ca. 418 °C. Similarly, TG curve of α-A-$[NBu^n_4]_3[PW_9O_{34}(CH_3SiO)_3(CH_3Si)]$ also exhibits two stages weight loss. The first weight loss of 23.43% occurs between 366.7 and 425.1 °C, corresponding to the loss of organic ammonium (calc. 22.90%); the second weight loss of 2.19% occurs between 425.1 and 520.0 °C, resulting from the loss of methyl group (calc. 2.14%). Two endothermal peaks are observed at 374.0 and 394.2 °C (assigned as C–Si cracked) in DTA curve. A stronger exothermal peak is observed in DTA curve at 407.6 °C, which could arise from the decomposition of the framework of **2**. These results illustrate that the framework of the complex **2** decomposes at ca. 407 °C.

2.5. X-ray diffraction and crystal structure

Diffraction quality crystals can be grown from DMF solvent at room temperature. Selected bond lengths (Å) and bond angles (°) are given in Table 2 for **1** and Table 3 for **2**. Figs. 1 and 2 illustrate the structures of the anions in the two compounds, together with the labeling scheme, respectively. The line drawing of **2** is shown in Fig. 3.

Table 2
Selected bond lengths (Å) and angles (°) for compound **1**

Bond lengths			
W(1)–O(1)	1.718(12)	W(1)–O(16)	1.888(11)
W(1)–O(14)	1.908(11)	W(1)–O(33)	1.919(11)
W(1)–O(36)	1.937(14)	W(1)–O(22)	2.362(10)
W(2)–O(2)	1.709(9)	W(2)–O(28)	1.869(11)
W(2)–O(29)	1.890(12)	W(2)–O(17)	1.903(11)
W(2)–O(33)	1.920(11)	W(2)–O(22)	2.386(9)
W(3)–O(3)	1.677(10)	W(3)–O(26)	1.864(11)
W(3)–O(17)	1.888(10)	W(3)–O(34)	1.912(10)
W(3)–O(20)	1.920(13)	W(3)–O(11)	2.352(9)
P(1)–O(22)	1.512(10)	P(1)–O(27)	1.513(10)
P(1)–O(11)	1.525(10)	P(1)–O(25)	1.531(10)
Si(1)–O(32)	1.527(13)	Si(1)–O(37)	1.633(14)
Si(1)–O(18)	1.641(13)	Si(1)–C(1)	1.79(3)
Si(2)–O(39)	1.637(16)	Si(2)–O(32)	1.665(13)
Si(2)–O(38)	1.681(16)	Si(2)–C(3)	1.81(2)
Bond angles			
O(32)–Si(1)–O(37)	111.5(7)	O(32)–Si(1)–O(18)	110.1(7)
O(37)–Si(1)–O(18)	107.9(6)	O(32)–Si(1)–C(1)	107.2(12)
O(37)–Si(1)–C(1)	110.3(11)	O(18)–Si(1)–C(1)	109.9(11)
O(39)–Si(2)–O(32)	109.5(7)	O(39)–Si(2)–O(38)	107.0(8)
O(32)–Si(2)–O(38)	108.3(7)	O(39)–Si(2)–C(3)	108.9(10)
O(32)–Si(2)–C(3)	113.8(10)	O(38)–Si(2)–C(3)	109.1(12)

Symmetry transformations used to generate equivalent atoms: #1 Y, Z, X; #2 Z, X, Y.

Table 3
Selected bond lengths (Å) and angles (°) for compound **2**

Bond lengths			
P(1)–O(22)	1.515(14)	P(1)–O(14)	1.524(15)
P(1)–O(5)	1.547(13)	P(1)–O(10)	1.553(14)
W(3)–O(34)	1.970(16)	W(5)–O(24)	1.931(17)
W(6)–O(16)	1.925(17)	W(7)–O(15)	1.920(17)
W(8)–O(23)	1.948(15)	W(9)–O(29)	1.892(18)
Si(1)–O(32)	1.58(2)	Si(1)–O(31)	1.614(18)
Si(1)–O(33)	1.62(2)	Si(2)–O(32)	1.61(2)
Si(2)–O(34)	1.630(18)	Si(2)–O(16)	1.658(18)
Si(3)–O(33)	1.59(2)	Si(3)–O(15)	1.650(18)
Si(3)–O(29)	1.674(19)	Si(4)–O(31)	1.584(18)
Si(4)–O(24)	1.62(2)	Si(4)–O(23)	1.640(17)
Bond angles			
O(32)–Si(1)–O(33)	108.8(12)	O(31)–Si(1)–O(33)	108.7(10)
O(32)–Si(1)–O(31)	112.0(11)	O(32)–Si(1)–C(4)	111.9(14)
O(31)–Si(1)–C(4)	107.8(13)	O(33)–Si(1)–C(4)	107.3(14)
O(32)–Si(2)–O(34)	110.7(10)	O(32)–Si(2)–O(16)	107.2(10)
O(34)–Si(2)–O(16)	108.0(9)	O(32)–Si(2)–C(2)	108.3(14)
O(34)–Si(2)–C(2)	110.1(13)	O(16)–Si(2)–C(2)	112.4(13)
O(33)–Si(3)–O(15)	111.0(9)	O(33)–Si(3)–O(29)	111.3(10)
O(15)–Si(3)–O(29)	107.1(9)	O(33)–Si(3)–C(3)	110.3(13)
O(15)–Si(3)–C(3)	108.7(12)	O(29)–Si(3)–C(3)	108.3(12)
O(31)–Si(4)–O(24)	110.5(10)	O(31)–Si(4)–O(23)	113.2(10)
O(24)–Si(4)–O(23)	107.0(9)	O(31)–Si(4)–C(1)	107.7(12)
O(24)–Si(4)–C(1)	112.2(13)	O(23)–Si(4)–C(1)	106.2(12)

The structure of anion **1** consists of one α-A-PW_9, four C_2H_3Si groups and three bridging O atoms (linked Si atom). α-A-PW_9 is grafted by three C_2H_3SiO groups through six Si–O–W bridges. On the other hand, each of three chemically equivalent C_2H_3SiO units is attached to the fourth C_2H_3Si through Si–O–Si bridges. The anion is close cage structure and displays C_{3v} symmetry which is different from that of anion α-A-$[PW_9O_{34}({}^{t}BuSiOH)_3]^{3-}$ [13] which is open, saturated cage structure by formation of six Si–O–W bridges connecting three organosilyl groups RSi.

In the structure of anion **1**, Si atoms, which act as the filling in the vacant of α-A-$PW_9O_{34}^{9-}$, have tetrahedron coordination. There is different distorted among the Si tetrahedra because of their different surroundings. The distortion of Si(2) tetrahedron is vigorous. The bond angles are in the range of 107.0(8)–113.8(10)°. The distortion of Si(1) tetrahedron is slight, the bond angles of the tetrahedron are in the range of 107.2(12)–111.5(7)°. The bond distances of Si(1)–O and Si(2)–O are also different. The bond distances of Si(1)–O are 1.527(13), 1.633(14), 1.641(13) Å, respectively. The average is 1.600 Å, the bond distances of Si(2)–O are 1.637(16), 1.665(13), 1.681(16) Å, the average is 1.661 Å. The average bond distance of Si(1)–O is 0.061 Å shorter than the bond distance of Si(2)–O. The longer bond distance of and more vigorous distortion of Si(2) tetrahedron may result from the special position. The PO_4 tetrahedron of anion **1** is slightly distorted in the compound due to one group of W_3O_{13} replaced.

The structure of anion **2** is also a close cage structure. It consists of one α-A-$PW_9O_{34}^{9-}$ anion, four CH_3SiO groups and three bridging O atoms. The α-A-$PW_9O_{34}^{9-}$ anion is grafted by three CH_3SiO groups through six Si–O–W bridges. On the other hand, each of three chemically equivalent CH_3SiO units is attached to the fourth CH_3Si through Si–O–Si bridges. The anion also displays C_{3v} symmetry.

In the structure of anion **2**, Si atoms, which fill the vacant of α-A-$PW_9O_{34}^{9-}$ anion are also tetrahedron coordination. The tetrahedra have all been slightly distorted (bond angles from 106.2(12) to 113.2(10)°) and the bond distances of Si–O(Si) are 1.62(2), 1.58(2), 1.61(2), 1.614(18), 1.59(2) and 1.584(18) Å, the average is 1.60 Å, the bond distances of Si–O(W) are 1.658(18), 1.674(19), 1.640(17), 1.630(18), 1.650(18) and 1.62(2) Å, with an average Si–O(W) bond length 1.645 Å. The Si–O(Si) bond distances (1.58–1.62 Å, average 1.60 Å) are somewhat shorter than those for Si–O(W) (1.62–1.674 Å, average 1.645 Å).

2.6. ^{31}P-NMR characterization

Each ^{31}P-NMR spectrum presents one line (Fig. 4a and b). Integration was carried out on proton-coupled spectra, with interpulse delays allowing full relaxation of the nuclei. The low-frequency resonance ($\delta = 16.680$ for **1**, 17.022 for **2**) is assigned to the central PO_4 tetrahedron of the polyoxotungstate [11]. This chemical shift, which is lower than that of the starting anion ($\delta = 5$, in

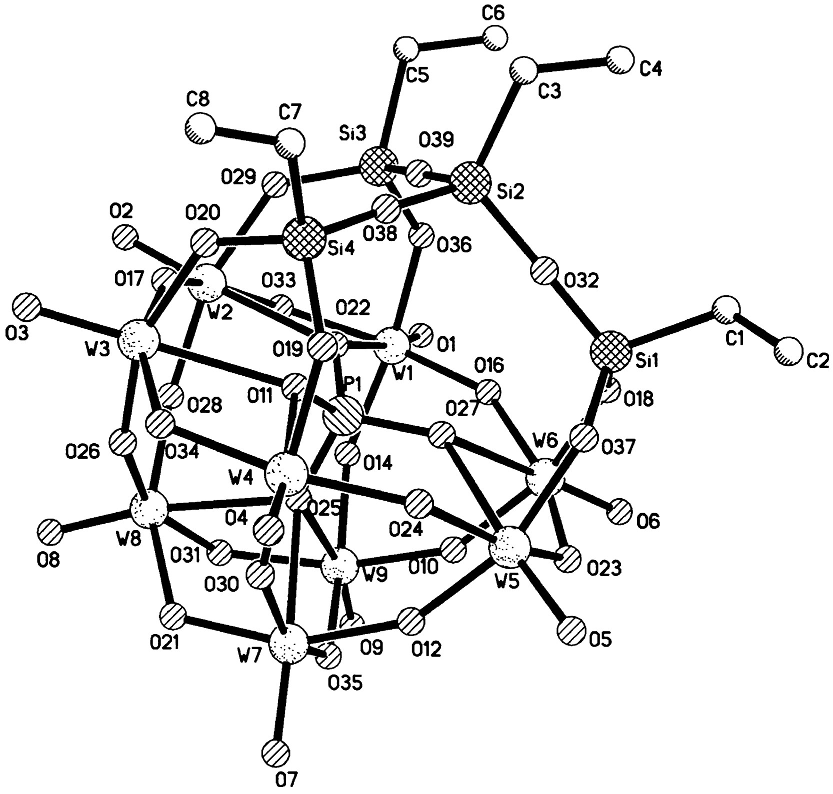

Fig. 1. Crystal structure of the title heteropolyanion **1**.

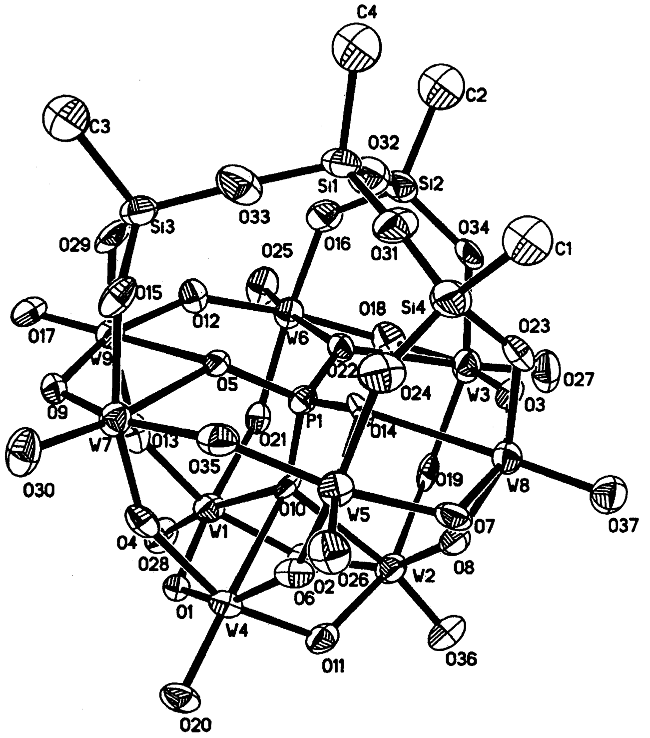

Fig. 2. Crystal structure of the title heteropolyanion **2**.

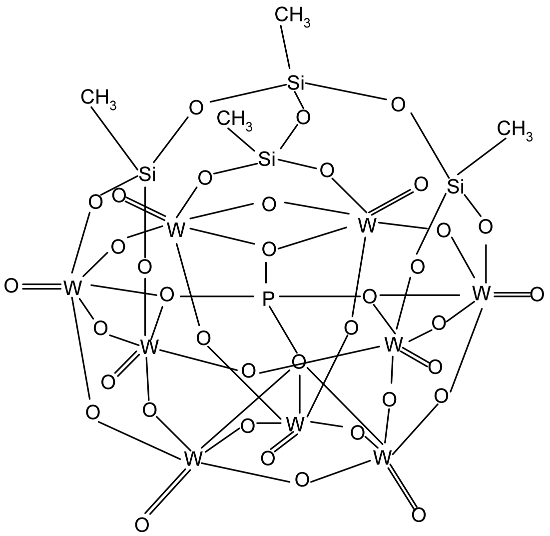

Fig. 3. The line drawing of the title anion **2**.

the solid state), is consistent with a partially saturated tungstophosphate structure [11,16]. ^{31}P-NMR spectra of **1** and **2** confirm that the conclusion of IR spectra and the single crystal X-ray diffraction analysis are consistent.

3. Experimental

3.1. General

The compound β-A-$Na_8H[PW_9O_{34}]\cdot 24\ H_2O$ was prepared according to the literature [21] and confirmed

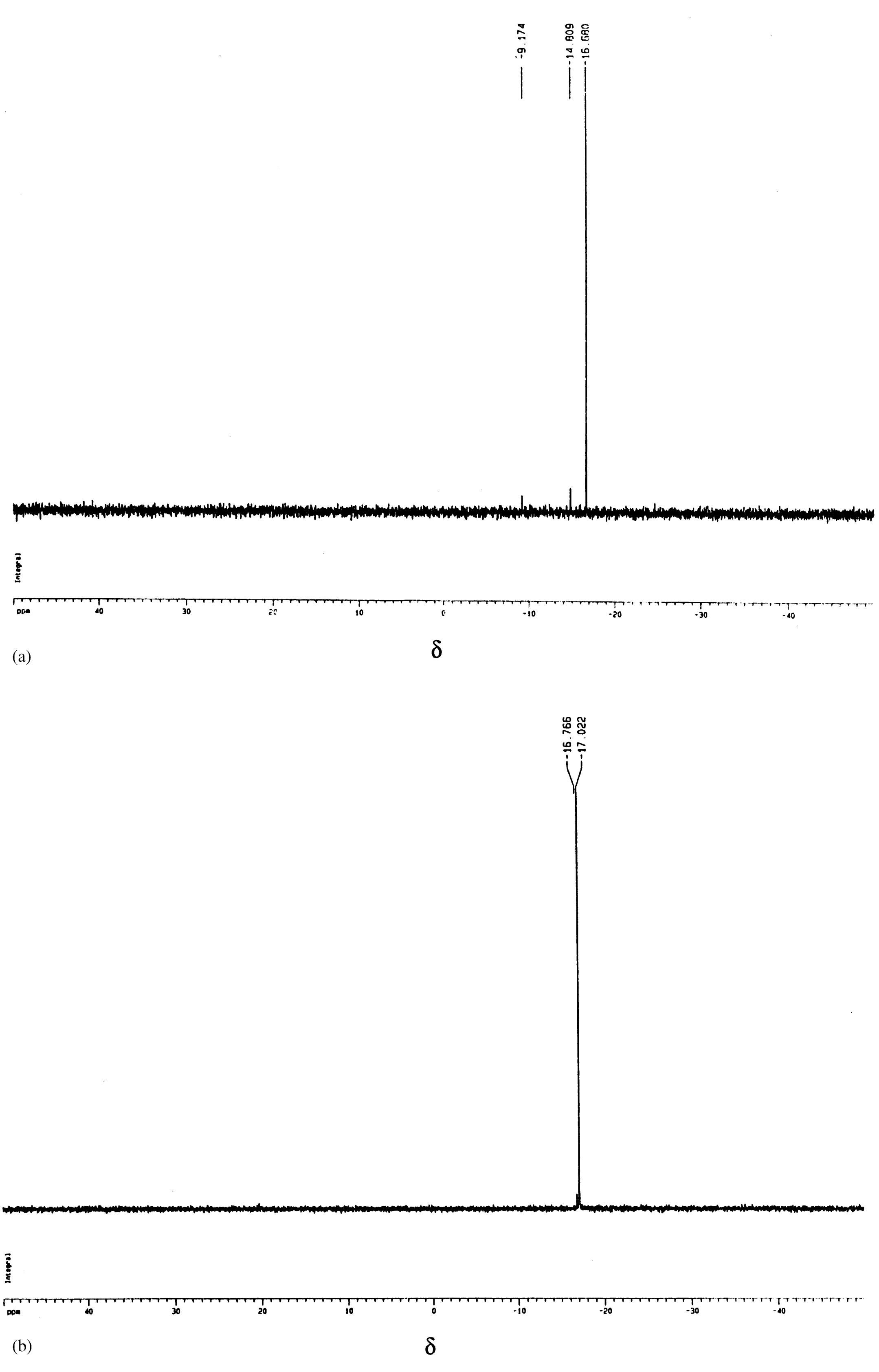

Fig. 4. (a) A ^{31}P-NMR spectrum of **1** in DMSO [$(CD_3)_2SO$]; (b) A ^{31}P-NMR spectrum of **2** in DMSO [$(CD_3)_2SO$].

by IR spectroscopy. Organosilicon trichloride $RSiCl_3$ [$R = C_2H_3$, CH_3] was from Across and was used as received. Other reagents were of analytical or guaranteed quality and were used as received without further purification. The elements were determined by the following methods: C, H and N elemental analyses were performed on a Perkin–Elmer 240C elemental analyzer; silicon was determined volumetrically with potassium fluorosilicate; tungsten was precipitated with cinchonin and weighted as WO_3 after heating the precipitate at 600 °C.

IR spectra were recorded on a Nicolet 170 SXFT-IR spectrometer using KBr pellets in 4000–400 cm^{-1}; UV spectra were obtained on a Shimazu UV–250 spectrophotometer (solvent acetonitrile); TG-DTA curves were obtained with Perkin–Elmer-7 instrument under air atmosphere with a heating rate of 10 °C min^{-1}, the reference material was α-alumina. ^{31}P-NMR spectra at room temperature (r.t.) in 5 mm outside diameter tubes were recorded on a Bruker DRX-500 spectrometer equipped with a QNP probehead. The chemical shifts are given according to the IUPAC convention, with respect to 85% H_3PO_4.

3.2. Preparations

3.2.1. α-A-$[NBu^n_4]_3[PW_9O_{34}(C_2H_3SiO)_3(C_2H_3Si)]$ (1)

The compounds β-A-$Na_8H[PW_9O_{34}]\cdot 24\ H_2O$ (2.87 g, 1 mmol) and NBu^n_4Br (1 g, ca. 3 mmol) were suspended in CH_3CN (60 ml); $C_2H_3SiCl_3$ (0.36 ml, 3 mmol) was added dropwise under vigorous stirring; the mixture was stirred 24 h at 0 °C. After separation of the white solid (NaCl + NaBr + traces of β-A-$Na_8H[PW_9O_{34}]\cdot 24\ H_2O$), colorless compound α-A-$[NBu^n_4]_3[PW_9O_{34}(C_2H_3SiO)_3(C_2H_3Si)]$ was formed by evaporation of the resulting solution at r.t. Crystals of α-A-$[NBu^n_4]_3[PW_9O_{34}(C_2H_3SiO)_3(C_2H_3Si)]$ suitable for single crystal structure determination were obtained upon slow evaporation of DMF solution of the compound. Anal. Calc. for $C_{56}H_{120}N_3O_{37}PSi_4W_9$: C, 20.95; H, 3.74; N, 1.31; Si, 3.49; W, 51.58. Found: C, 20.90; H, 3.81; N, 1.41; Si, 3.47; W, 51.51%.

3.2.2. α-A-$[NBu^n_4]_3[PW_9O_{34}(CH_3SiO)_3(CH_3Si)]$ (2)

This compound was similarly synthesized from β-A-$Na_8H[PW_9O_{34}]\cdot 24\ H_2O$ (2.87 g, 1 mmol), CH_3CN (60 ml), NBu^n_4Br (1 g, ca. 3 mmol), CH_3SiCl_3 (0.36 ml, 3 mmol). After separation of the white solid (NaCl + NaBr + traces of β-A-$Na_8H[PW_9O_{34}]\cdot 24\ H_2O$), the white compound α-A-$[NBu^n_4]_3[PW_9O_{34}(CH_3SiO)_3(CH_3Si)]$ was formed by evaporation of the resulting solution at r.t. Single crystals of α-A-$[NBu^n_4]_3[PW_9O_{34}(CH_3SiO)_3(CH_3Si)]$ were obtained upon slow evaporation of DMF solution of the compound. Anal. Calc. for $C_{52}H_{120}N_3O_{37}PSi_4W_9$: C, 19.64; H, 3.78; N, 1.32; Si, 3.52; W, 52.08. Found: C, 19.60; H, 4.15; N, 1.53; Si, 3.62; W, 52.30%.

3.3. Single crystal X-ray diffraction analyses

Suitable size single crystals of the title compounds were obtained upon slow evaporation of DMF solution of the compounds at r.t. Crystals of compound **1** having approximate dimensions of 0.24 × 0.22 × 0.18 mm were mounted on a glass fiber. Crystals of compound **2** having approximate dimensions of 0.28 × 0.24 × 0.18 mm were mounted on a glass fiber. All measurements were made on a Rigaku RAXIS-IV image plate area detector with graphite monochromated Mo–K_α radiation. The structures were solved by direct methods and expanded using Fourier techniques. The nonhydrogen atoms were refined anisotropically. Hydrogen atoms were included but not refined. The final cycle of full-matrix least-squares refinement was based on 24511 observed reflections [$I > 2\sigma(I)$] and 713 variable parameters for **1** and 27042 observed reflections [$I > 2\sigma(I)$] and 682 variable parameters for **2**. All calculations were performed using the SHELXL-97 program [22]. Crystal data, together with the diffraction data collection and

Table 4
Crystal data, collection parameters, and refinements for complexes **1** and **2**

Complexes	**1**	**2**
Empirical formula	$C_{56}H_{120}N_3O_{39}PSi_4W_9$	$C_{52}H_{120}N_3O_{37}PSi_4W_9$
Formula weight	3207.39	3177.09
Temperature (K)	293(2)	293(2)
Crystal color and form	colorless, needle	colorless, needle
Space group	$Pca2_1$	$Pca2_1$
Crystal system	orthohombic	orthohombic
a (Å)	26.548(5)	25.761(5)
b (Å)	14.423(3)	14.519(3)
c (Å)	24.387(5)	24.396(5)
V (Å^3)	9338(3)	9124(3)
Z	4	4
D_{calc} (Mg m^{-3})	2.281	2.225
Absorption coefficient (mm^{-1})	11.181	11.438
$F(000)$	5968	5464
Crystal size (mm)	0.24 × 0.22 × 0.18	0.28 × 0.24 × 0.18
θ_{max} (°)	25.50	27.53
Number of collected reflections	24511	27042
Number of independent reflections	14489	10198
Number of parameters	713	682
Goodness-of-fit	1.025	
Final R indices [$I > 2.00\sigma(I)$]	$R = 0.0500$, $wR = 0.0928$	$R = 0.0561$, $wR = 0.1100$
R indices (all data)	$R = 0.0681$, $wR = 0.0979$	$R = 0.0866$, $wR = 0.1196$
Largest differential peak and hole (e Å^{-3})	0.867 and −1.015	1.328 and −2.011

structure refinement parameters for compounds **1** and **2** are presented in Table 4.

4. Supplementary material

Crystallographic data for structural analysis have been deposited with the Cambridge Crystallographic Data Center, CCDC nos. 192706 and 172610 for complexes **1** and **2**, respectively. Copies of this information may be obtained free of charge from The Director, CCDC, 12 Union Road, Cambridge, CB2 1EZ, UK (Fax: +44-1223-336033; e-mail: deposit@ccdc.cam.ac.uk or www: http://www.ccdc.cam.ac.uk).

Acknowledgements

This work was supported by the Nature Science Foundation of Henan Province and Outstanding Youth Foundation of Henan Province.

References

[1] M.T. Pope, Heteropoly and Isopoly Oxometalates, Springer–Verlag, Berlin, New York, 1983, p. 32.
[2] M.T. Pope, A. Müller, Angew. Chem. Int. Ed. Engl. 103 (1991) 56.
[3] C.L. Hill, Coord. Chem. Rev. 143 (1995) 407.
[4] J.T. Rhule, C.L. Hill, D.A. Judd, R.F. Schinazi, Chem. Rev. 98 (1998) 327.
[5] J. Thygesen, S. Weinstein, F. Franceschi, A. Yonath, Structure 4 (1996) 513.
[6] J. Thygesen, A. Yonath, et al., J. Cryst. Growth. 168 (1996) 308.
[7] W.H. Knoth, P.J. Domaille, R.D. Farlee, Organometallics 4 (1985) 62.
[8] F. Xin, M.T. Pope, Organometallics 13 (1994) 4881.
[9] F. Xin, M.T. Pope, G.J. Long, U. Russo, Inorg. Chem. 35 (1996) 1207.
[10] G. Sazani, M.H. Dickman, M.T. Pope, Inorg. Chem. 39 (2000) 939.
[11] C.R. Mayer, R. Thouvenot, J. Chem. Soc. Dalton Trans. (1998) 7.
[12] A. Mazeaud, Y. Dromzee, R. Thouvenot, Inorg. Chem. 39 (2000) 4735.
[13] C.R. Mayer, V. Cabuil, T. Lalot, R. Thouvenot, Angew. Chem. Int. Ed. 38 (1999) 3672.
[14] C.R. Mayer, R. Thouvenot, T. Lalot, Chem. Mater. 12 (2000) 257.
[15] C.R. Mayer, R. Thouvenot, T. Lalot, Macromolecules 33 (2000) 4433.
[16] A. Mazeaud, N. Ammari, F. Robert, R. Thouvenot, Angew. Chem. Int. Ed. Engl. 35 (1996) 1961.
[17] A. Mazeaud, Y. Dromzee, R. Thouvenot, Inorg. Chem. 39 (2000) 4735.
[18] C. Rocchiccioli-Deltcheff, M. Fournier, R. Franck, R. Thouvenot, Inorg. Chem. 22 (1983) 207.
[19] J.F. Liu, Z. Liu, E.B. Wang, L.Y. Qu, Acta Chimica Sinica 49 (1991) 782.
[20] C. Rocchiccioli-Deltcheff, R. Thouvenot, R. Franck, Spectrochim. Acta Part A 32 (1975) 587.
[21] R. Massart, R. Constant, J.M. Fruchart, J.P. Ciabrini, M. Fournier, Inorg. Chem. 16 (1977) 2916.
[22] G.M. Sheldrick, SHELXL-97: Program for Crystal Structure Refinement, University of Göttingen, Germany, 1997.